Korea-Australia Rheology Journal
Vol. 22, No. 4, December 2010 pp. 331-338

Capillary breakup extensional rheometry of semi-dilute polymer solutions

Christian Clasen*
Department of Chemical Engineering, Katholieke Universiteit Leuven, W. de Croylaan 46, 3001 Heverlee, Belgium
(Received May 25, 2010; accepted June 11, 2010)

Abstract

In this paper the thinning and breakup of filaments of semi-dilute solutions of polystyrene in diethyl phthalate is investigated with a capillary breakup extensional rheometer. The solutions show a long initial visco-capillary balance that can be fitted with 0-D Newtonian and power law models. The onset of the elasto-capillary balance is molecular weight dependent and the coil stretch transition of the polymer is shifted close to the breaking point and to small filament diameters. However, the transition is even for concentrations up to c/c* ~ 30 observable due to a strong extension thinning in the Caber experiment. It is shown that the transition to the elasto-capillary balance takes place at local elasto-capillary number $Ec^* = 4.7$ that incorporates the extensional relaxation time λ_E and the extension thinning viscosity $\eta_{E,app}$.

Keywords **:** extensional rheology, semi-dilute solution, extension thinning, relaxation time, elasto-capillary number, capillary breakup, polystyrene, Caber

1. Introduction

The determination of the longest relaxation time λ_E of a viscoelastic fluid in an uniaxial extensional flow field is one of the main applications of the capillary breakup extensional rheometry. While for dilute polymer solutions quantitative predictions of the thinning dynamics of a liquid filament are possible (Anna and McKinley, 2001; Plog *et al.,* 2005; Clasen, Eggers *et al.,* 2006; Clasen, Plog *et al.,* 2006; Kojic *et al.,* 2006; Yesilata *et al.,* 2006; Rothstein *et al.,* 2008; Clasen *et al.,* 2009; Miller *et al.,* 2009), for semi-dilute to concentrated solutions even qualitative models are lacking (McKinley, 2005) and only empirical relations of the material functions in extension are reported (Stelter *et al.,* 2002; Wagner, 2010).

One further problem with the determined of a relaxation time from the thinning curves of semi-dilute to concentrated polymer solutions is that Caber results are often misinterpreted and that the exponential fits to the data in the elasto-capillary thinning are not correctly done. The inexperienced user is expecting to observe an exponential thinning regime as high polymer concentrations imply a strong elastic component (but is not aware of a delayed onset of the elasto-capillary balance regime due to an also high viscosity). Unfortunately the shape of the thinning curve with an initially slow thinning in the Newtonian regime and an accelerated thinning in a power-law regime resembles in a log-lin representation the shape of an exponential thinning regime of a (dilute) Boger fluid that reaches its finite extensibility limit (and that have been used extensively in the past to investigate the Caber technique (Anna and McKinley, 2001; Anna *et al.,* 2001; Rothstein and McKinley, 2002; Larson, 2005; Plog *et al.,* 2005)). However, since the transition from a visco-capillary balance to an elasto-capillary balance (that shows an exponential filament decay) is shifting with increasing concentrations to smaller filament radii, often regions that do not represent elastic thinning are fitted.

Within this paper we want therefore to establish a criterion for when and where semi-dilute and concentrated polymer solutions will show an elasto-capillary thinning in a Caber type experiment, and how reliable relaxation times λ_E can be extracted.

2. Materials and Methods

The fluid investigated were solutions of poly(styrene) standards (Polymer Laboratories, Amherst, MA, USA) in diethyl phthalate (DEP) (Merck, Darmstadt, Germany) with weight average molecular weights of $M_w = 1.87 \cdot 10^6$ g/mol (later on labeled as PS2), $M_w = 3.84 \cdot 10^6$ g/mol (labeled as PS4), $M_w = 7.11 \cdot 10^6$ g/mol (labeled as PS7) and $M_w = 13.2 \cdot 10^6$ g/mol (labeled as PS13).

Capillary thinning experiments were conducted with a Caber 1 (Thermo Fisher Scientific, Karlsruhe, Germany), using circular endplates with a diameter of $D_p = 6$ mm diameter and an initial aspect ratio of $\Lambda_f = h_0/D_p = 0.5$ (where h_0 is the initial plate distance). The fluid was carefully filled in the gap between the endplates to form a cylindrical bridge with diameter D_p. The plates were then separated to a final

*Corresponding author: christian.clasen@cit.kuleuven.be

aspect ratio of $\Lambda_f = h_0/D_p = 1.3$ within 50 ms, and the subsequent evolution of the filament diameter with time was monitored with the laser micrometer of the Caber. Special care was taken to correct the data with the laser-micrometer readout *after* the filament was broken to assure the necessary accuracy of diameter data at the micrometer level.

The rheology of the test fluids in both steady and dynamic shear flow was investigated with an ARES rheometer (TA Instruments, Newcastle DE, USA) with cone and plate fixtures of 40 mm diameter and a cone angle of 0.04 rad.

Intrinsic viscosities $[\eta]$ where determined with an Ubbelohde capillary to $[\eta] = 283$ cm^3/g for PS2 2, $[\eta] = 351$ cm^3/g for PS4, $[\eta] = 464$ cm^3/g for PS7 and $[\eta] = 601$ cm^3/g for PS13, resulting in critical concentrations $c^* = 0.77/[\eta]$ (Graessley, 1980) of $c^* = 0.27\%$ for PS2, $c^* = 0.22\%$ for PS4, $c^* = 0.17\%$ for PS7, and $c^* = 0.13\%$ for PS13.

Surface tensions γ were determined with a Wilhelmy balance.

3. Results

As shown in Fig. 1 for the solution of PS4, one can observe pronounced differences in the thinning dynamics of a polymer solution when increasing the concentration. Whereas for a low concentration of 0.316% (which is close to the critical concentration of $c^* = 0.22\%$ for PS4) the thinning is dominated by a long exponential regime, this regime is getting smaller for higher concentrations. This is shown in more detail in Fig. 2 for a concentration of 5%. The observed thinning of a filament of a semi-dilute polymer solution in Figure can be separated into four regions:

Regime **I** is an ill-defined thinning profile that still contains strong contributions of gravitational sagging. A local Bond number can be used to define a lower boundary to this regime

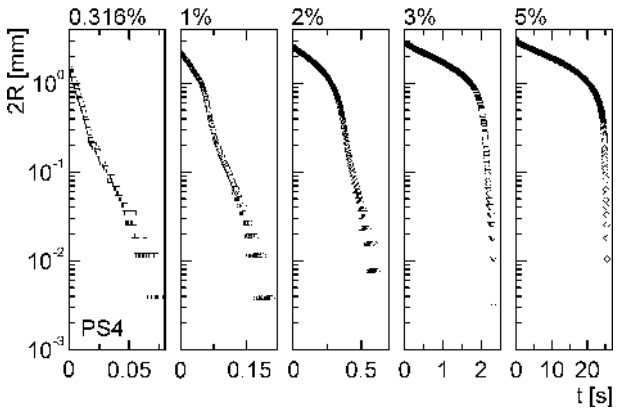

Fig. 1. Evolution of the mid filament diameter $2R$ as function of time t for solutions of polystyrene PS4 (M_w=3.84·10^6 g/mol) in diethylphthalate at five different concentrations.

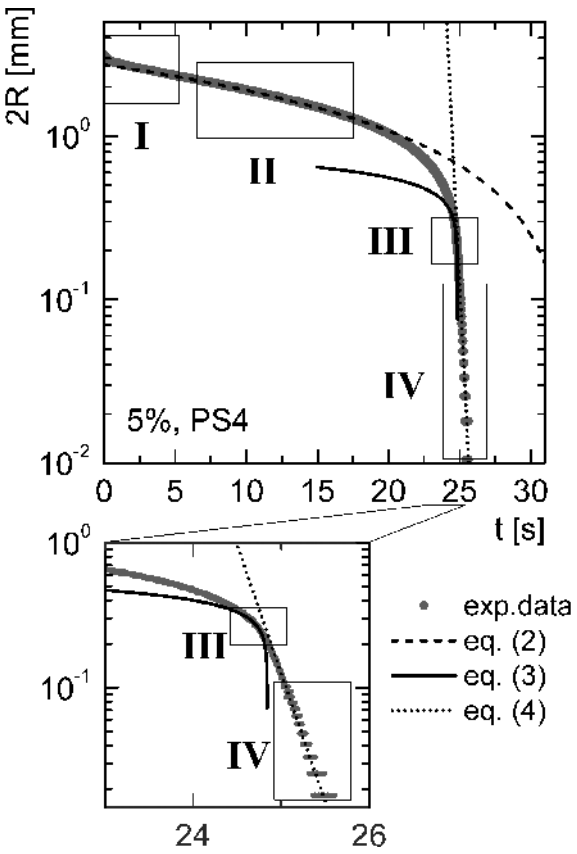

Fig. 2. Evolution of the mid filament diameter $2R$ as function of time t for a 5 wt% solution of polystyrene PS4 (M_w = 3.84·10^6 g/mol) in diethylphthalate.

$$Bo^* = \frac{\rho g R^2}{\gamma} \tag{1}$$

with the density ρ, gravitational constant g, surface tension γ and the local filament radius R(t) that decreases with time. By experience gravitational effects can be neglected for local Bond number below ~0.2 which in the present case calculates to a radius of ~1 mm.

Regime **II** sets in below this critical Bond number and is controlled by a visco-capillary balance of the capillary pressure γ/R and the viscous stresses $\eta_E \dot{\varepsilon}$ in the filament. Since the filament radius is still large, the extension rate $\dot{\varepsilon}$ is low enough so that a Newtonian thinning regime with a constant Trouton ratio of the extensional viscosity η_E to the zero-shear viscosity η_0 of $\eta_E/\eta_0 = 3$ is observed. The radius evolution can in this regime be described with the similarity solution of Papageorgiou (Papageorgiou, 1995; McKinley and Tripathi, 2000)

$$R = 0.0709 \frac{\gamma}{\eta}(t_b - t)\,. \tag{2}$$

Here t_b refers to the breakup time of the filament and η is the shear viscosity. A fit of eq. (2) to the experimental data

in Fig. 2 in regime II is indicated by the dashed line, using the zero-shear viscosity η_0 determined from the flow curve.

Regime **III** is still showing a visco-capillary balance, however, the surface pressure and hence the extension rate $\dot{\varepsilon}$ is high enough so that the polymer solution is showing an extensional thinning, originating from the increased disentanglement and orientation of the polymer chains as described by Keunings *et al*. (Bousfield *et al.*, 1986). For an extensional viscosity that follows in this regime a power law of the form $\eta_E = K\dot{\varepsilon}^{n-1}$ with a power law exponent n between 0 and 1 the filament diameter evolves as (Doshi *et al.*, 2003)

$$R = \Phi\frac{\gamma}{K}(t_b - t)^n, \tag{3}$$

where the numerical front factor Φ is a function of n (Doshi *et al.*, 2003; McKinley, 2005; Suryo and Basaran, 2006). In Fig. 2 a fit of the power law regime with eq. (3) is shown as a straight line, with the power law exponent n taken from the shear thinning regime of the flow curve of the steady shear experiment that follows $\eta = K\dot{\gamma}^{n-1}$. In the transitional regime between II and III the viscosity is already decreasing, but has not reached the power law thinning yet.

Regime **IV** is showing then the onset of an elasto-capillary balance where the surface pressure is balanced by the elastic stresses of the unraveling polymer chains. Within the elasto-capillary balance regime the filament is decaying exponentially with time (Entov and Hinch, 1997; Anna and McKinley, 2001; Clasen, Eggers *et al.,* 2006; Clasen, Plog *et al.*, 2006)

$$R = R_0\left(\frac{GR_0}{2\gamma}\right)^{\frac{1}{3}} e^{\frac{-t}{3\lambda_E}}. \tag{4}$$

The inset in Fig. 2 allows to better observe the exponential thinning in regime IV that only takes place at small diameters close to breakup, and that also shows good agreement with the exponential thinning of eq. (4). For concentrated solutions the onset of finite extensibility effects in regime IV close to the breaking point has been reported (McKinely *et al.,* 2001), but is not occurring within the observable range of the current investigation.

It is possible to also calculate an extensional viscosity from the thinning data of Fig. 2. Although the deformation history in capillary breakup experiment is complex and the conformation of the polymers in solution is not reaching a steady state, one can still formulate an apparent extensional viscosity $\eta_{E,app} = \gamma/(R\dot{\varepsilon})$, assuming that the stress in the fluid is equal to the surface pressure γ/R. The extension rate is directly obtained from the evolution of the filament radius as

$$\dot{\varepsilon} = -\frac{2}{R}\frac{dR}{dt} \tag{5}$$

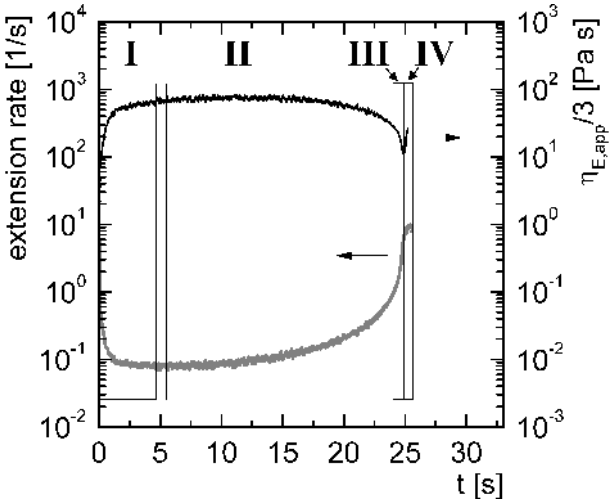

Fig. 3. Extension rate $\dot{\varepsilon}$ and apparent extensional viscosity $\eta_{E,app}$ evolution in a capillary breakup experiment for a solution of polystyrene PS4 ($M_w = 3.84{\cdot}10^6$ g/mol) in diethylphthalate, determined from the thinning data of Fig. 2 via eq. (5) and (6).

which results in an apparent extensional viscosity

$$\eta_{E,app} = \frac{\gamma}{2\frac{dR}{dt}}. \tag{6}$$

In Fig. 3 both extension rate and apparent extensional viscosity are plotted as a function of time for the thinning data of Fig. 2. As expected the viscosity is constant within the indicated regime II while the extension rate rises. Approaching regime III the viscosity is decreasing while the extension rate is further increasing. Directly after regime III when reaching regime IV the extension rate is suddenly approaching a constant value while the viscosity shows a sharp increase. This is more obvious when plotting the apparent extensional viscosity $\eta_{E,app}$ directly as a function of the extension rate $\dot{\varepsilon}$ as shown in Fig. 4. The initial decrease in extension rate and increase in viscosity in the ill-defined regime I is not representing actual material functions but originating from the gravitational sagging. In this representation the power law thinning (regime III) is directly observable, as well as the constant extension rate in regime IV. The constant extension rate is directly related to the relaxation time λ_E that the solution is exhibiting in an uniaxial extensional flow via $\dot{\varepsilon} = 2/(3\lambda_E)$, which can be obtained by inserting eq. (4) into eq. (5) (Entov and Hinch, 1997).

It is obvious from the radius evolution of Fig. 2 that the onset of the elastic thinning regime IV for a semi-dilute polymer solution is only happening at late times close to the breaking point and at small radii. In order to do a good fit of regime IV at filament radii of order O(50 μm) and

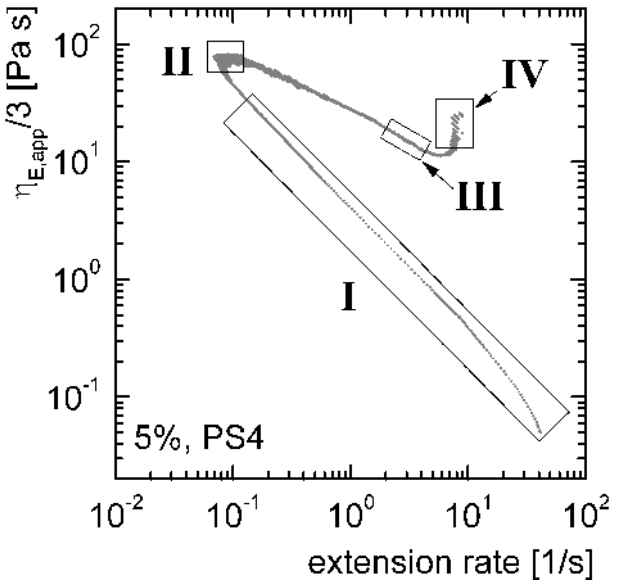

Fig. 4. Apparent extensional viscosity $\eta_{E,app}$ as a function of the extension rate $\dot{\varepsilon}$, data from Fig. 3.

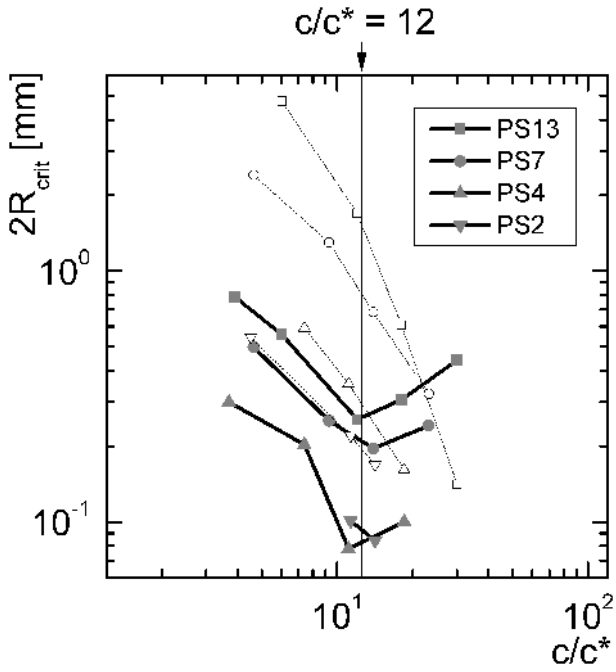

Fig. 5. Critical diameter $2R_{crit}$ (at which a transition from the visco-capillary to the elastocapillary balance is observed) as a function of the overlap parameter c/c^* for the different polystyrene in DEP solutions(closed symbols are experimental values, open symbols from eq. (10)).

below with eq. (4) (to extract a relaxation time), great care needs to be taken to determine the 'zero' diameter readout after the filament is broken and to correct the experimental diameters with this offset. Several incorrect exponential fits in this regime have been published. These fits are then often close to the actual relaxation time, since the slope of the extension thinning regime III close to the transition to the elasto-capillary thinning in regime IV are by definition similar. This has been leading to some misinterpretations, in particular when relating to shear relaxation times.

In order to quantify the effect of polymer concentration on the radius at which the transition from regime III to IV is observed Fig. 5 shows the critical radii R_{crit} at which this transition takes place (closed symbols). Plotting this radius as function of the overlap parameter c/c^* indicates that R_{crit} is first decreasing with increasing concentration and has a minimum value around $c/c^* \sim 12$. At higher overlap concentrations R_{crit} is not further decreasing with increasing concentration, but levels off and even shows a slight increase. Still, the critical radii at higher concentrations are of order O(100 μm) and below. It requires therefore careful experiments in order to evaluate an exponential thinning below these critical radii and the resolution limit of the filament radius often hinders a quantitative evaluation at all (Regev *et al.,* 2010).

Another observation that can be made from Fig. 5 is that with decreasing molecular weight M_w the transitional radii shift to even lower values.

It would be desirable to predict *a priori* if a semi-dilute or concentrated polymer solution will show an elasticity controlled thinning regime IV at filament radii that are still within the experimental window of a capillary breakup experiment. For dilute solutions a prediction of the onset point of elasticity can be done quantitatively as shown in (Campo-Deano and Clasen, 2010). For more concentrated solutions one could compare the timescales of the timescales of the thinning dynamics II and IV in order to predict where for a given polymer solution the transition from regime III to IV takes place (and if this is still in the observable range of the experiment). The elasto-capillary number introduced by McKinley *et al*. (Anna and McKinley, 2001)

$$Ec = \frac{\lambda\gamma}{\eta R_0} \tag{7}$$

compares the timescale of an elasticity controlled thinning (the relaxation time λ) with the viscous timescale $\eta R_0/\gamma$ that gives the time to breakup of a filament that would thin only in regime II. An elasto-capillary number $Ec \gg 1$ indicates then an overall elasticity dominated thinning, controlled by the relaxation time λ, whereas $Ec \ll 1$ points to a viscosity controlled thinning that is determined by the ratio η/γ. Using the initial radius R_0 as the characteristic length scale we can now calculate an overall elasto-capillary number for each polymer and concentration, using the zero-shear viscosity and the terminal relaxation time $\lambda = \lim_{\omega\to 0} G'/(G''\omega)$ obtained from oscillatory shear experiments. As it can be seen in Fig. 6 the elasto-capillary number Ec (open symbols) is decreasing with an increasing concentration. This is counterintuitive since one instinc-

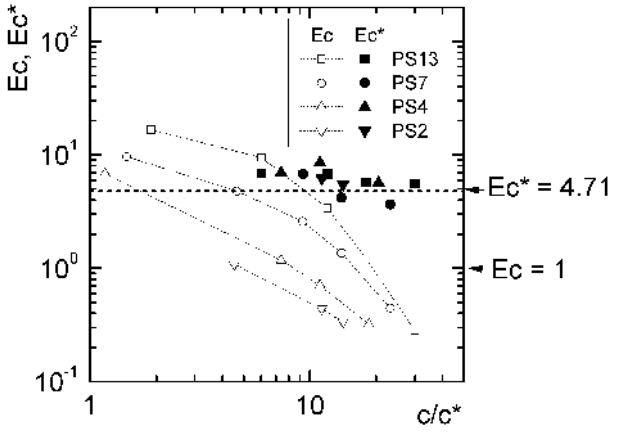

Fig. 6. Elastocapillary number *Ec* of eq. (7) (open symbols), and local elastocapillary number *Ec** from eq. (8) (filled symbols) as a function of the overlap parameter c/c* for the different polystyrene in DEP solutions.

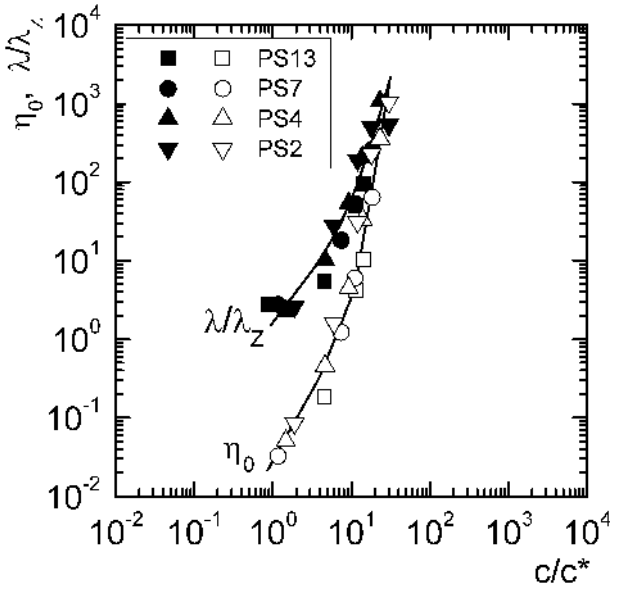

Fig. 7. Zero-shear viscosity η_0 (open symbols), and terminal relaxation time λ from oscillatory shear experiments (normalized with the Zimm relaxation time λ_Z) (closed symbols), as a function of the overlap parameter c/c* for the different polystyrene in DEP solutions.

tively expects stronger elastic effects and higher relaxation times with increasing concentration. However, viscosity increases too and stronger then the relaxation time. This can be seen in Fig. 7 that gives the zero-shear viscosities η_0 obtained from the steady shear, and the terminal relaxation time λ obtained from oscillatory shear experiments (and scaled with the Zimm relaxation time λ_Z to obtain a master curve (Clasen, Plog *et al.,* 2006)). From this it becomes obvious that the elasto-capillary number will decrease with concentration (at least in the concentration range investigated in this study).

At lower concentrations the elasto-capillary number evolves in the same direction as the critical radius in Fig. 5. This is expected as with increasing concentration the portion of regime IV in comparison to regime II is decreasing and consequently also the radius R_{crit} at which the transition takes place.

However, using now an *Ec* number of unity as a criterion to judge if an elastic thinning regime IV is observable or not, Fig. 6 predicts that there should be no observable elastic thinning for higher concentrations. In contrast to this Figs. 2-5 indicate that even at the highest investigated concentrations a transition to an elastic thinning regime IV is still observable (although at very small filament diameters and at the experimental limits). The reason for this apparent discrepancy is that the global elasto-capillary number is only indicating which thinning regime is going to dominate the overall thinning behaviour initially and over most of the time. As it can be seen for the example shown in Fig. 2, for which the elasto-capillary number calculates to *Ec* = 0.44, it is obvious that the viscosity controlled thinning regime II (and III) are dominating over most of the time. Still, even a short elasticity controlled thinning regime as shown in the inset of Fig. 2 can allow extracting a relaxation time if sufficient data is within the experimentally accessible filament diameter range. Although capturing the general trend, the elasto-capillary number alone is therefore not sufficient to indicate if a regime IV is observable.

In order to better describe the transition to the elastic thinning regime, one can use a local elasto-capillary number *Ec** that uses the actual radius $R(t)$ and that develops therefore with time

$$Ec^* = \frac{\lambda\gamma}{\eta R(t)} \tag{8}$$

Outgoing from the equations (2) and (4) for the radius evolution in the regimes II and IV one can obtain via the first derivatives the thinning velocities $U = -dR/dt$ as $U_\eta = 0.0709(\gamma/\eta)$ for regime II and $U_\lambda = R/(3\lambda)$ for regime IV. Formulating the local elasto-capillary number from the ratio of these velocities (rather than as a ratio of timescales) we obtain the appropriate numerical front factor that describes the correct transitional value for the local elasto-capillary number

$$\frac{U_\eta}{U_\lambda} = 0.2127\frac{\lambda\gamma}{\eta R(t)} = \frac{Ec^*}{4.7015} \tag{9}$$

We can now rewrite this to obtain the radius at which the local elasto-capillary number reaches the critical value *Ec** = 4.7015:

$$R_{crit} = 0.2127\frac{\lambda\gamma}{\eta} \tag{10}$$

In Fig. 5 these theoretical radii (open symbols) are compared to the experimentally observed ones. Obviously the theoretical values of eq. (10) are overestimating the experimentally observed values and also do not capture the leveling of the observed radii above an overlap concentration of $c/c^* = 12$.

The main reason for this discrepancy is the fact that for the calculation of R_{crit} via eq. (10) we still used the terminal relaxation time λ and viscosity η_0 obtained from the steady and oscillatory shear experiments. However, the shear relaxation time is different from the actual relaxation time λ_E in an extensional flow field, and λ_E cannot be predicted from shear experiments. For dilute polymer solutions λ_E has shown to be larger than the shear relaxation times (Bazilevskii *et al.,* 2001; Clasen, Plog *et al.,* 2006; Tirtaatmadja *et al.,* 2006). For semi-dilute to concentrated solutions λ_E can actually be shorter than λ. Investigations on capillary thinning of concentrated solutions indicated that the relaxation time scales are actually closer to the Rouse time then to the longest reptation time scale (Bhattacharjee *et al.,* 2003).

A comparison of the terminal relaxation times λ with λ_E obtained from the fitting exponential thinning regime of the capillary breakup experiments is done in Fig. 8 (both relaxation times are scaled with the respective Zimm relaxation times λ_Z in order to allow for a better visualization of the different molecular weights (Clasen, Plog *et al.,* 2006)). It is obvious that for the investigated concentration range λ_E is not as strongly increasing with the concentration c/c^* as λ and furthermore that λ_E is smaller than λ. Therefore using the shear relaxation time in eq. (8) is overestimating Ec^* and gives therefore too high values for R_{crit}.

However, also the extensional viscosities η_E are not the same as the viscosities η in steady shear. As for example shown by Bhattacharjee *et al*. (Bhattacharjee *et al.,* 2002; Bhattacharjee *et al.,* 2003) the steady state extensional viscosity of entangled polymer solutions can be larger as well as smaller than the respective value $\eta_{E,0} = \eta_0/3$ for a Newtonian liquid with the same shear viscosity η_0. Furthermore, during the filament thinning process the polymer solution is experiencing different extension rates and has a complex evolution of the (transient) viscosity that cannot be related to steady state values. The apparent viscosity $\eta_{E,app}$ of eq. (6) represents this transient experienced by the thinning filament. Comparing now the experimentally observed apparent viscosities of the Caber experiment with the steady state shear viscosities as a function of the deformation rate in Fig. 9, it can be seen that for a lower concentration of 2% η and $\eta_{E,app}$ show the same values and deformation rate thinning. However, for the higher concentrations (3% and 5%) the onset of rate thinning sets in at much lower deformation rates in the Caber experiment. Following that, the apparent extensional viscosity that the higher concentrated polymer solutions are experiencing at

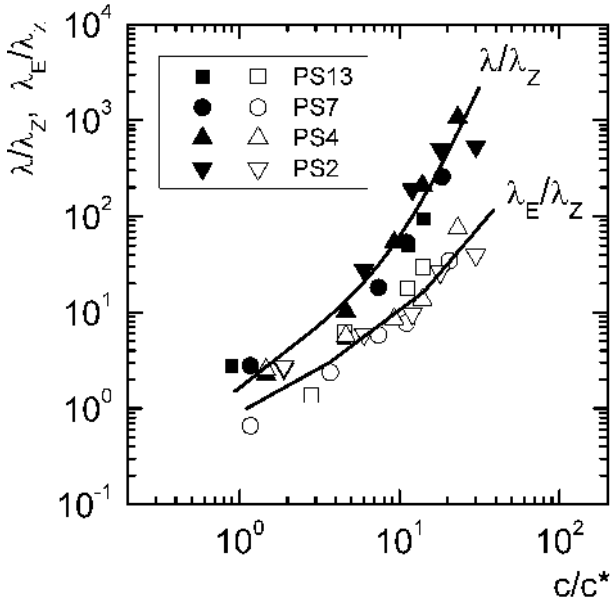

Fig. 8. Comparison of the terminal relaxation time λ from oscillatory shear experiments with the extensional relaxation time λ_E experiments (both normalized with the Zimm relaxation time λ_Z).

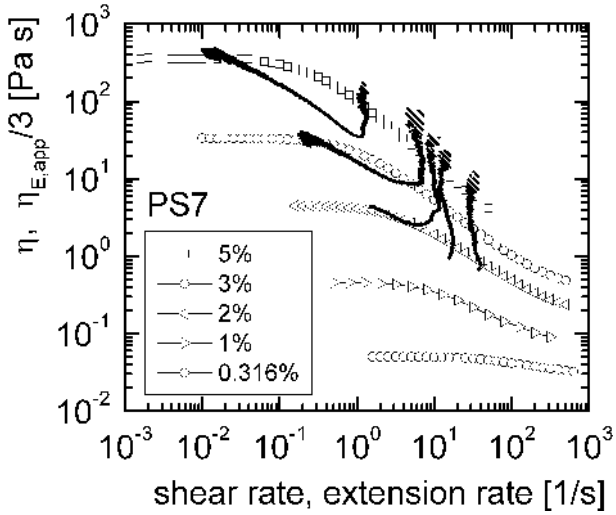

Fig. 9. Comparison of the steady shear viscosity η as a function of the shear rate $\dot{\gamma}$ (open symbols), with the transient, apparent extensional viscosity $\eta_{E,app}$ as a function of the extension rate $\dot{\varepsilon}$ (small filled symbols) for solutions of polystyrene PS7 ($M_w = 7.11 \cdot 10^6$ g/mol) in diethylphthalate at five different concentrations.

the onset of regime IV is much lower than the shear viscosity (even when taking into account the rate dependent thinning of the shear viscosity).

This strong extension thinning is the reason why we observe in Fig. 5 the leveling off of the experimental crit-

ical radius R_{crit} above $c/c^* \sim 12$. Lowering the viscosity that enters eq. (8) will lead to higher critical radii. The possibility to observe an elasticity controlled thinning regime IV even for the higher concentrations originates therefore in the pronounced extension thinning that the apparent extensional viscosity is showing.

A strong indication that it is indeed the local elasto-capillary number Ec^* that determines the transition to regime IV can be obtained when using all the actually experimental parameters at the onset of the exponential thinning regime. With the experimental critical radii of Fig. 5, the relaxation times in extension from Fig. 8 and the extensional viscosity at the onset of regime IV (from Fig. 9) we can do a quantitative calculation of the local elasto-capillary number Ec^* via eq. (8). The results in Fig. 6 show that the actual values of Ec* at the transition are independent of concentration or molecular weight and close to the critical value of 4.7.

Unfortunately there is at this moment no quantitative theory that would allow to predict the evolution of the material functions in the extensional flow field of the Caber that enter the local elasto-capillary number of eq. (8). The Giesekus model could provide in numerical simulations a qualitative description of the response of entangled polymer solutions in a transient extensional flow (Yao *et al.,* 1998; Yao *et al.,* 2000), but no analytic solution that could deliver the required input for eq. (8).

Still, even using the shear values to calculate a rough estimation for the overall elasto-capillary number Ec allows to estimate if the thinning dynamics will show a pronounced regime IV and the possibility of an easy extraction of a relaxation time (for $Ec \gg 1$), or if for $Ec \sim 1$ the critical limit is reached where an elastic regime IV is barely observable and a relaxation time λ_E can only be obtained for high molecular weights and only with great experimental care.

Acknowledgments

The author acknowledges financial support of this project from the ERC-2007-StG starting grant 203043 NANOFIB.

References

Anna, S.L. and G.H. McKinley, 2001, Elasto-capillary thinning and breakup of model elastic liquids, *J. Rheol.* **45**(1), 115-138.

Anna, S.L., G.H. McKinley, D.A. Nguyen, T. Sridhar, S.J. Muller, J. Huang and D.F. James, 2001, An interlaboratory comparison of measurements from filament- stretching rheometers using common test fluids, *J. Rheol.* **45**(1), 83-114.

Bazilevskii, A.V., V.M. Entov and A.N. Rozhkov, 2001, Breakup of an Oldroyd liquid bridge as a method for testing the rheological properties of polymer solutions, *Vysokomolekulyarnye Soedineniya Seriya A* **43**(7), 716-726.

Bhattacharjee, P.K., D.A. Nguyen, G.H. McKinley and T. Sridhar, 2003, Extensional stress growth and stress relaxation in entangled polymer solutions, *J. Rheol.* **47**(1), 269-290.

Bhattacharjee, P.K., J.P. Oberhauser, G.H. McKinley, L.G. Leal and T. Sridhar, 2002, Extensional rheometry of entangled solutions, *Macromolecules* **25**, 10131-10148.

Bousfield, D.W., R. Keunings, G. Marrucci and M.M. Denn, 1986, Nonlinear-analysis of the surface-tension driven breakup of viscoelastic filaments, *J. Non-Newton. Fluid Mech.* **21**(1), 79-97.

Campo-Deano, L. and C. Clasen, 2010, The slow retraction method (SRM) for the determination of ultra-short relaxation times in capillary breakup experiments, *J. Non-Newton. Fluid Mech.* **165**, 1688-1699.

Clasen, C., J. Bico, V.M. Entov and G.H. McKinley, 2009, 'Gobbling drops': the jetting-dripping transition in flows of polymer solutions, *J. Fluid Mech.* **636**, 5-40.

Clasen, C., J. Eggers, M.A. Fontelos, J. Li and G.H. McKinley, 2006, The beads-on-string structure of viscoelastic threads, *J. Fluid Mech.* **556**, 283-308.

Clasen, C., J.P. Plog, W.M. Kulicke, M. Owens, C. Macosko, L.E. Scriven, M. Verani and G.H. McKinley, 2006, How dilute are dilute solutions in extensional flows?, *J. Rheol.* **50**(6), 849-881.

Doshi, P., R. Suryo, O.E. Yildirim, G.H. McKinley and O.A. Basaran, 2003, Scaling in pinch-off of generalized newtonian fluids, *J. Non-Newton. Fluid Mech.* **113**(1), 1-27.

Entov, V.M. and E.J. Hinch, 1997, Effect of a spectrum of relaxation times on the capillary thinning of a filament of elastic liquid, *J. Non-Newton. Fluid Mech.* **72**(1), 31-53.

Graessley, W.W., 1980, Polymer chain dimensions and the dependence of viscoelasic properties on the concentration, molecular weight and solvent power, *Polymer* **21**(3), 258-262.

Kojic, N., J. Bico, C. Clasen and G.H. McKinely, 2006, Ex-vivo rheology of spider silk, *Journal of Experimental Biology* **209**, 4355-4362.

Larson, R.G., 2005, The rheology of dilute solutions of flexible polymers: Progress and problems, *J. Rheol.* **49**(1), 1-70.

McKinely, G.H., O. Brauner and M.W. Yao, 2001, Kinematics of Filament Stretching in Dilute and Concentrated Polymer Solutions, *Korea-Aust. Rheol. J.* **13**, 29-35.

McKinley, G.H., 2005, Visco-elasto-capillary thinning and breakup of complex fluids, *Rheology Reviews*, 1-48.

McKinley, G.H. and A. Tripathi, 2000, How to extract the Newtonian viscosity from capillary breakup measurements in a filament rheometer, *J. Rheol.* **44**(3), 653-670.

Miller, E., C. Clasen and J.P. Rothstein, 2009, The effect of step-stretch parameters on capillary breakup extensional rheology (CaBER) measurements, *Rheol. Acta* **48**(6), 625-639.

Papageorgiou, D.T., 1995, On the breakup of viscous-liquid threads, *Phys. Fluids* **7**(7), 1529-1544.

Plog, J.P., W.M. Kulicke and C. Clasen, 2005, Influence of the molar mass distribution on the elongational behaviour of polymer solutions in capillary breakup, *Appl. Rheol.* **15**(1), 28-37.

Regev, O., S. Vandebril, E. Zussman and C. Clasen, 2010, The role of interfacial viscoelasticity in the stabilization of an elec-

trospun jet, *Polymer* **51**, 2611-2620.
Rothstein, J.P. and G.H. McKinley, 2002, Inhomogeneous transient uniaxial extensional rheometry, *J. Rheol.* **46**(6), 1419-1443.
Rothstein, J.P., E. Miller, P. Moldenaers and C. Clasen, 2008, The effect of step-stretch parameters on capillary breakup extensional rheology (CaBER) measurements, Amer Inst Physics, Melville.
Stelter, M., G. Brenn, A.L. Yarin, R.P. Singh and F. Durst, 2002, Investigation of the elongational behavior of polymer solutions by means of an elongational rheometer, *J. Rheol.* **46**(2), 507-527.
Suryo, R. and O.A. Basaran, 2006, Local dynamics during pinch-off of liquid threads of power law fluids: Scaling analysis and self-similarity, *J. Non-Newton. Fluid Mech.* **138**(2-3), 134-160.
Tirtaatmadja, V., G.H. McKinley and J.J. Cooper-White, 2006, Drop formation and breakup of low viscosity elastic fluids: Effects of molecular weight and concentration, *Phys. Fluids* **18**(4).
Wagner, C., 2010, Is there a relation between the relaxation time measured in CaBER experiments and the first normal stress coefficient?, *J. Non-Newton. Fluid Mech.* **165**, 1265-1274.
Yao, M.W., G.H. McKinley and B. Debbaut, 1998, Extensional deformation, stress relaxation and necking failure of viscoelastic filaments, *J. Non-Newton. Fluid Mech.* **79**(2-3), 469-501.
Yao, M.W., S.H. Spiegelberg and G.H. McKinley, 2000, Dynamics of weakly strain-hardening fluids in filament stretching devices, *J. Non-Newton. Fluid Mech.* **89**(1-2), 1-43.
Yesilata, B., C. Clasen and G.H. McKinley, 2006, Nonlinear shear and extensional flow dynamics of wormlike surfactant solutions, *J. Non-Newton. Fluid Mech.* **133**(2-3), 73-90.